ROYAL SOCIETY OF CHEMISTRY

EDGE ARTICLE

Check for updates

Oxidation-induced nucleophilic substitution at the electron-rich B(12) vertex in [CB₁₁H₁₂]⁻ under catalyst-free conditions†

Wanqi Sun,‡[a] Yujie Jin,‡[ab] Yongtao Wang, [ID] *[ab] Zeyu Wen, [ID] [a] Jizeng Sun,[a] Jia Yao, [ID] [ab] Simon Duttwyler [ID] [a] and Haoran Li [ID] *[abc]

Highly regioselective B(12) substitutions of the monocarborane anion [CB₁₁H₁₂]⁻ has been a challenge. Here, we synthesized a stable B−O−N zwitterionic compound with an impressive yield (isolated yield up to 98%) and excellent regioselectivity at the B(12) position under catalyst-free conditions. The kinetics, substituent effect, and capture experiments are paired with theoretical calculations, showing that the reaction mechanism is oxidation-induced nucleophilic substitution. The hydride anion at the B(12) position is abstracted by an oxoammonium oxidant with lower cleavage energy of 4.2 kcal mol⁻¹ than B(7−11) positions, thereby changing the electronegativity upon the conversion of [CB₁₁H₁₂]⁻ to neutral [CB₁₁H₁₁], in turn giving very high regioselectivity for nucleophilic substitution. This work presents an effective method for synthesizing B(12) oxygen derivatives of the [CB₁₁H₁₂]⁻ anion.
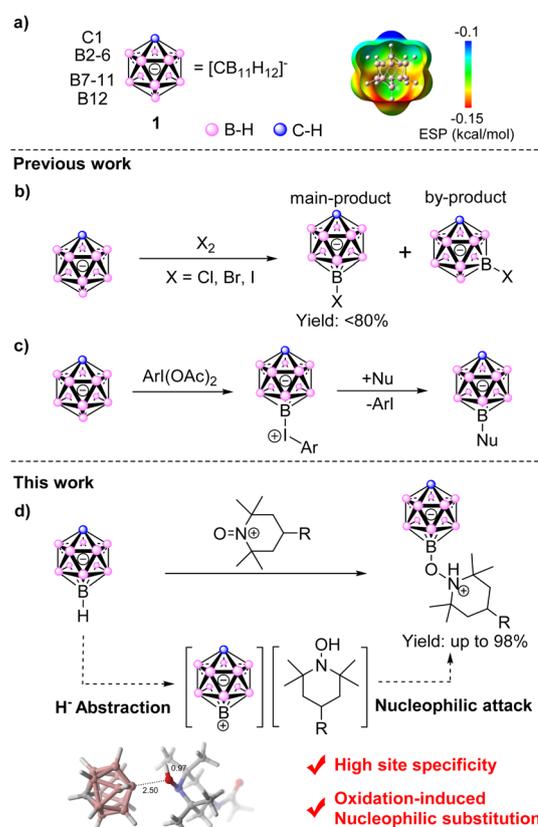
Introduction

12-Vertex boron clusters, characterized by their distinctive icosahedral geometry and exceptional stability,[1–4] have garnered significant attention across diverse fields.[5–14] Monocarborane anion [CB₁₁H₁₂]⁻, with a single negative charge, has received particular attention.[15–18] Highly regioselective B(12) substitutions are a challenge due to the minimal polarization and high symmetry of the B–H bond.[19–23] Currently, there are two mechanisms for achieving monosubstitution at the B(12) position of [CB₁₁H₁₂]⁻. (1) Electrophilic substitution, the electrophilic halogenation is most commonly used.[24–26] However, 7-isomers were always obtained as by-products due to the similar electrostatic potential at B(7–11) to that at B(12) (Fig. 1a). The less regioselective electrophilic substitutions commonly cause lower yields (Fig. 1b). (2) Nucleophilic substitution, boron-centered cations were generally proposed to be key intermediates in the chemistry of polyhedral boron hydrides,[27–29] however, limited studies are reported on the functionalization of [CB₁₁H₁₂]⁻. Hydroxylation at the B(12) position using 80% sulfuric acid yields 12-hydroxy anions under elevated

Fig. 1 (a) The monocarborane anion [CB₁₁H₁₂]⁻ and electrostatic potential surface; (b) previously reported electrophilic substitution; (c) previously reported nucleophilic substitution; (d) overview and summary of the key finding in this work.

[a]Department of Chemistry, Zhejiang University, 866 Yuhangtang Rd, Hangzhou 310058, China. E-mail: wyongtao@zju.edu.cn; lihr@zju.edu.cn

[b]Center of Chemistry for Frontier Technologies, ZJU-NHU United R&D Center, Zhejiang University, 866 Yuhangtang Rd, Hangzhou 310058, China

[c]State Key Laboratory of Chemical Engineering, College of Chemical and Biological Engineering, Zhejiang University, 866 Yuhangtang Rd, Hangzhou 310058, China

† Electronic supplementary information (ESI) available. CCDC 2407119–2407122. For ESI and crystallographic data in CIF or other electronic format see DOI: https://doi.org/10.1039/d5sc00234f

‡ These authors contributed equally: Wanqi Sun and Yujie Jin.

temperatures.[30] Electrophile-induced nucleophilic substitution (EINS)[31] has been proposed for this reaction.[32,33] Recently, Kaszyński and co-workers found that $[CB_{11}H_{12}]^-$ reacts with iodobenzene diacetate, yielding zwitterionic products Ar-I$^+$-$[CB_{11}H_{11}]^-$ at the B(12) position, which undergo nucleophilic substitution to generate a series of functionalized derivatives of the $[CB_{11}H_{12}]^-$ anion (Fig. 1c).[34,35]

Oxoammonium salts are commonly utilized as oxidants in organic synthesis for their easy access and recyclability,[36–41] and they are commonly used as hydride abstracting reagents.[42,43] For example, they catalyze the oxidation of alcohols or ether to yield the corresponding aldehydes, ketones, or carboxylic acids *via* a hydrogen anion abstraction mechanism.[44] Recently, Lin and co-workers achieved the oxidation of ethers to lactones with the oxoammonium cation, where the hydride abstraction from C–H was also suggested.[45]

Inspired by these literature studies, we hypothesized that oxoammonium salts might also abstract hydride from B–H bonds in $[CB_{11}H_{12}]^-$. As expected, we found a novel coupling reaction of oxoammonium salts and $[CB_{11}H_{12}]^-$ to form stable B–O–N compounds under catalyst-free conditions. This approach exhibited excellent regioselectivity with high B(12) substituted products. The reaction was found to undergo an oxoammonium oxidation-induced nucleophilic substitution (OINS) by various mechanistic studies, such as kinetic studies, substituent effects, EPR spectroscopy, trapping experiments, and theoretical calculations.

Results and discussion

At the very beginning, optimization of the reaction conditions was conducted (Table S1†). The conditions outlined in entry 12 of Table S1† were identified as optimal. The optimized reaction conditions were $[CB_{11}H_{12}]^-$ with 1.25 equivalents of the commercial agent $[AcNH\text{-}TEMPO]^+ [BF_4]^-$ in 1,4-dioxane at 80 °C for 180 min.

Under optimal conditions, a scale-up synthesis of **2** was carried out with a high isolated yield of 98%. The new compound was characterized through spectroscopic techniques, including ^1H, $^1H\{^{11}B\}$, ^{11}B, $^{11}B\{^1H\}$, and $^{13}C\{^1H\}$ NMR, as well as high resolution mass spectrometry (HRMS). The ^{11}B NMR spectra displayed a similar pattern of $1:5:5$ with the chemical shifts of B(12) vertices changed from $\delta = -7.93$ ppm to $\delta = 11.8$ ppm. Moreover, single crystals of the composition were obtained from an acetone solution *via* slow evaporation. And the single-crystal X-ray analysis of **2** confirms the molecular structure (Fig. 2b). For compound **2**, the observed distances are B12–O1 1.459 Å, O1–N1 1.423 Å, with an angle of B12–O1–N1 at 123.33°. The distances and angles are comparable to those reported in the previous literature.[46] In addition, the B–O–N compound is a zwitterionic compound with high stability.[47,48] The theoretically calculated dipole moment is 11.75.

In an effort to investigate the reaction mechanism behind such high regioselectivity, we performed density functional theory (DFT) calculations for the heterolytic cleavage of various B–H bonds in $[CB_{11}H_{12}]^-$. Due to the influence of H$^+$ or H$^-$
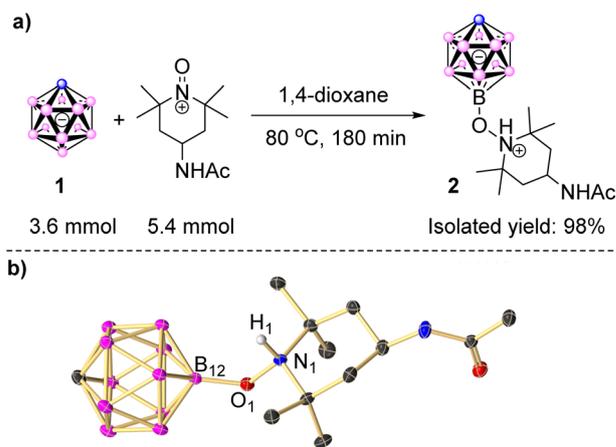

Fig. 2 (a) Gram-scale synthesis and (b) X-ray crystal structures of **2**. Cations and H atoms are omitted for clarity; 30% displacement ellipsoids.

acceptors on the value of Gibbs free energy change (ΔG), the relative Gibbs free energy change ($\Delta\Delta G$) was calculated in this work by subtracting ΔG with ΔG(B(12)–H) in $[CB_{11}H_{12}]^-$. $\Delta-H$ Fig. 3a presents the $\Delta\Delta G$, indicating that the B(12) position is the most favorable for H$^-$ loss, followed by B(7) and, ultimately, B(2). In contrast, the $\Delta\Delta G$ trend of losing H$^+$ is exactly opposite as the proton at B(2) was most activated. Given that the regioselectivity was favored at the B(12) site, it was more likely to undergo a hydride abstraction pathway. Simultaneously, we calculated the $\Delta\Delta G$ for various B–H bonds in $[CB_{11}H_{12}]^-$ analogues, including $[B_{12}H_{12}]^{2-}$ and $m\text{-}C_2B_{10}H_{12}$. By comparison, H$^-$ loss was easier in $[B_{12}H_{12}]^{2-}$, which lacks a carbon vertex, as the $\Delta\Delta G$ is -12.2 kcal mol^{-1}. However, it is more difficult for *meta*-carborane 1,7-$C_2B_{10}H_{12}$ to lose H$^-$ with $\Delta\Delta G$ of B–H in any position exceeding 20 kcal mol^{-1}. To check these calculation results, we carried out the experimental work, and found that neither *ortho*-C_2B_{10}, nor *meta*-C_2B_{10}, nor *para*-C_2B_{10} reacted with $[AcNH\text{-}TEMPO]^+[BF_4]^-$, and the single-substituted product could not be obtained in $[B_{12}H_{12}]^{2-}$. These verified that the reaction process involved the loss of H$^-$ rather than the loss of H$^+$.

Further evidence came from the fact that the compound did not react with $[AcNH\text{-}TEMPO]^+[BF_4]^-$ when the electron-withdrawing iodine substituent occupied position B(12). In contrast, the coupling product at position 7 (the second most likely position to lose H$^-$) was obtained with an isolated yield of 85% when the electron-donating effect $[12\text{-}CH_3\text{-}CB_{11}H_{11}]^-$ was used. Additionally, theoretical calculations indicated that the $\Delta\Delta G$ for H$^-$ loss at this position was reduced by 0.9 kcal mol^{-1} compared to $[CB_{11}H_{12}]^-$, which further proved that the reaction involved a hydride anion abstraction (H$^-$ loss) process. In addition, when electron-donating –CH$_3$ and electron-withdrawing –NHAc substituents were attached to the C vertex of $[CB_{11}H_{12}]^-$, the results were consistent with our expectations: the desired product was obtained with an isolated yield of 72% when $[1\text{-}CH_3\text{-}CB_{11}H_{11}]^-$ was used, whereas $[1\text{-}AcNH\text{-}CB_{11}H_{11}]^-$ did not undergo conversion (Fig. 3c).
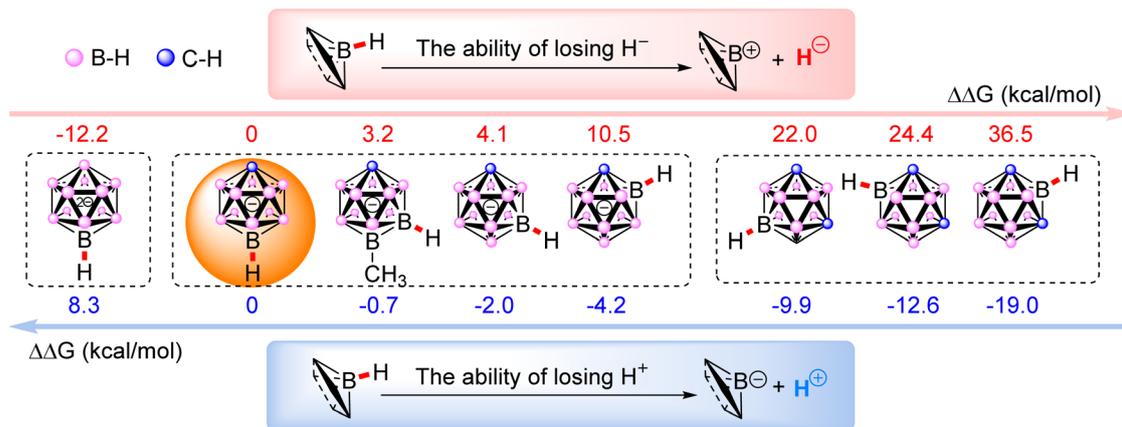
Fig. 3 (a) Relative Gibbs free energy change (ΔΔG) for the heterolytic cleavage of B–H bonds, showing the loss of H⁻ (red) and H⁺ (blue); (b) reactivity of different boron clusters and (c) reactivity of different substituents of the $[CB_{11}H_{12}]^-$ anion.

Subsequently, the transition state for B(12)–H heterolysis was investigated (Fig. 4a–c). Initially, we tried to find a 4-member ring type transition state to mediate concerted H-abstraction and B–O bond formation, but failed due to the large steric hindrance between the oxoammonium cation and the $[CB_{11}H_{12}]^-$ cage. However, a reasonable transition state was found for the transfer of H⁻ to O atom at the oxoammonium cation, and the intrinsic reaction coordinate (IRC) analysis

suggested the subsequent O–B bond formation after the formation of the $[CB_{11}H_{11}]$[hydroxylamine] pair. The corresponding activation Gibbs free energy $(\Delta G^{\ddagger})$ was 21.1 kcal mol⁻¹, owing a favored energy barrier of 4.2 kcal mol⁻¹ to that at the B(7–11) positions $(\Delta G^{\ddagger} = 25.3$ kcal mol⁻¹). The intrinsic bond orbitals (IBOs) along the reaction coordinate supported the hydride anion abstraction by the oxoammonium cation. As illustrated in Fig. 4b, apparent electron flow was observed from
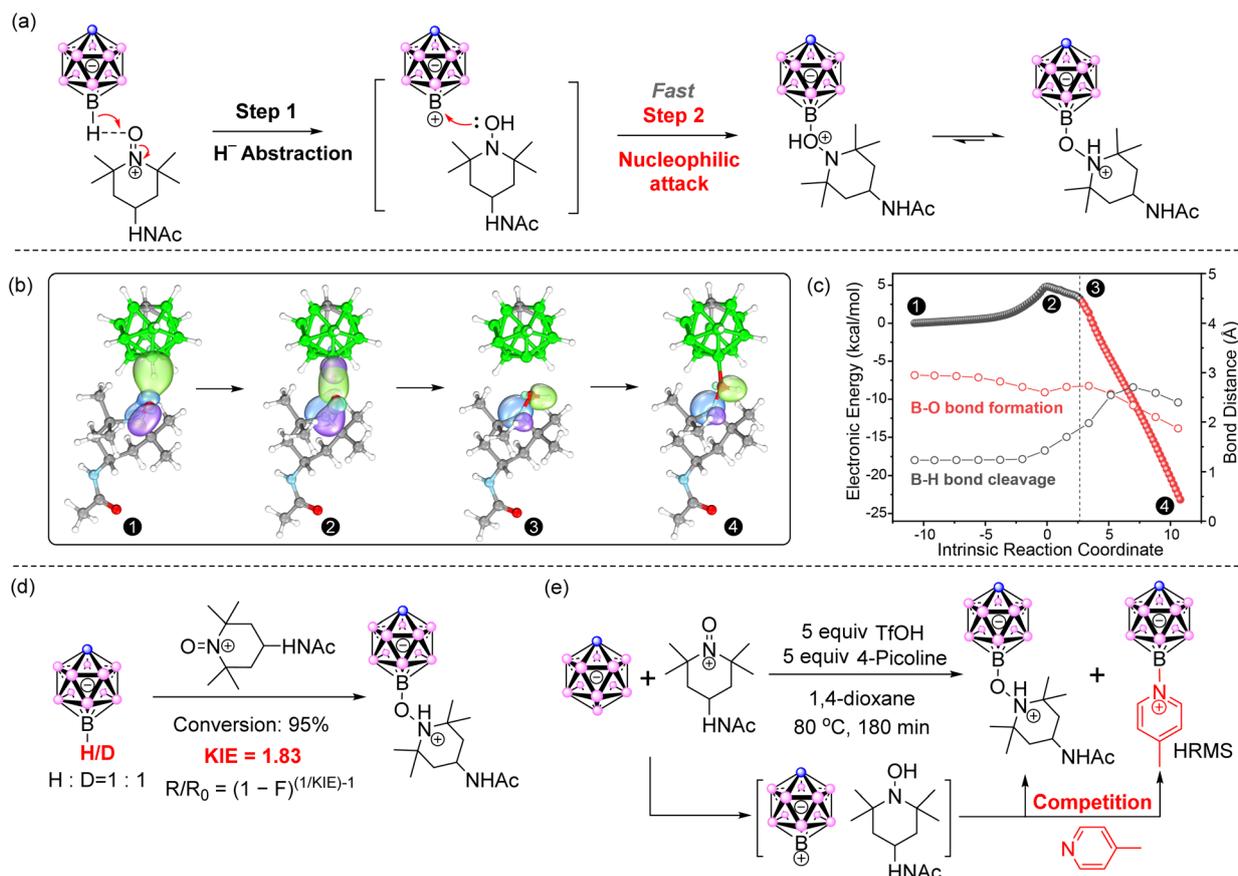
Fig. 4 (a) Proposed mechanism; (b) the intrinsic bond orbitals (IBOs) illustrate the electron flow during the reaction between $[CB_{11}H_{12}]^-$ and oxoammonium cation and proposed mechanism; (c) the change of electronic energies along the intrinsic reaction coordinate for the sequentially occurring step 1 (blank balls) and step 2 (red balls). The dotted lines indicate the change of B–H (black) and B–O (red) bond distances along the intrinsic reaction coordinate; (d) determination of KIE for B–H; (e) capture experiments.

the $[CB_{11}H_{12}]^-$ σ orbital to the NO π orbital and the transient intermediate $CB_{11}H_{11}$ and hydroxylamine were formed, indicating the apparent hydride anion transfer. Besides, the IRC plot indicated that this reaction proceeded in two steps and involved a high-energy transition state (Fig. 4c). In the first step, the H atom of $[CB_{11}H_{12}]^-$ moves toward the oxoammonium salts, resulting in B–H bond cleavage and O–H bond formation (blank balls). The B–O distance decreases from 2.95 to 2.60 Å. In the next step, starting from the red balls, hydroxylamine attacks the electrophilic intermediate, forming the final product. The B–O distance further decreases from 2.60 to 1.87 Å. The formation of the B–O–N coupling product was exergonic by 56.3 kcal mol^{-1}. Based on the above calculations, we propose the following mechanism: firstly, the $[CB_{11}H_{12}]^-$ is oxidized by $[AcNH\text{-}TEMPO]^+[BF_4]^-$ to form the paired intermediate, $[CB_{11}H_{11}][hydroxylamine]$. Subsequently, hydroxylamine, acting as a nucleophilic reagent, attacked the intermediate $CB_{11}H_{11}$ to form the B–O–N compound as the final product.

To support the proposed mechanism involving hydride abstraction and subsequently nuleophilic substitution, hydrogen kinetic isotope effect (KIE) experiments were conducted (Fig. 4d). $[H\text{-}CB_{11}D_{11}]^-$ was synthesized from $[CB_{11}H_{12}]^-$ *via* microwave reaction in D_2O containing 20 wt% DCl. A 1 : 1 reaction between

$[CB_{11}H_{12}]^-$ and $[H\text{-}CB_{11}D_{11}]^-$ was conducted under standard reaction conditions. At 95% conversion, an apparent KIE of 1.83 was calculated using the equation $R/R_0 = (1-F)^{(1/KIE)-1}$ (Fig. 4d).[49] In general, primary KIEs typically range from 2 to 8, while secondary KIEs fall within 1.0 to 1.2.[50] The observed KIE value of 1.83 is closer to the range of primary KIEs, suggesting that the cleavage of the B–H/D bond was the rate-determining step.

In addition, the radical pathway was excluded by the control experiment and electron paramagnetic resonance spectroscopy (EPR). The reaction could run the same way in the dark. The [AcNH-TEMPO] radical could not take the place of [AcNH-TEMPO]$^+$[BF$_4$]$^-$ to oxidize $[CB_{11}H_{12}]^-$ under standard conditions. No significant signals were detected during the reaction by EPR (Fig. S2†).

Next, in order to prove the nucleophilic step, 4-methylpyridine, a nucleophile, was introduced into the reaction and found to be attached to the $[CB_{11}H_{12}]^-$ anion in the presence of trifluoromethanesulfonic acid (Fig. S3†), which supported an S_N1 mechanism. Besides, the oxide form of 4-methylpyridine-*N*-oxide did not appear, excluding the 4-methylpyridine oxidation route. Furthermore, when 4-methylpyridine was replaced with 4-methoxypyridine, the product with 4-methoxypyridine attached to the $[CB_{11}H_{12}]^-$ anion was also observed in HRMS (Fig. S4†).

Water, acting as a nucleophile, was also employed in varying amounts to perform the capturing reaction. Anhydrous 1,4-dioxane, untreated commercial 1,4-dioxane, and 1,4-dioxane containing 10 v% water were used as solvents. HRMS data revealed an increasing ratio of hydroxyl-substituted $[CB_{11}H_{12}]^-$ anion to the hydroxylamine-substituted $[CB_{11}H_{12}]^-$ anion (Fig. S5–S7†). However, the yields of these captured compounds were relatively low, making isolation and precise determination of the ratio challenging. This could be attributed to the preferential reaction within the *in situ*-formed $[CB_{11}H_{11}]$ [hydroxylamine] pair, which suppresses competition from other nucleophiles. In brief, these experimental results demonstrated that the reaction proceeded in two steps, likely following an S_N1-type nucleophilic substitution mechanism rather than an S_N2. The oxidation of the B–H bond in $[CB_{11}H_{12}]^-$ by oxoammonium salts leads to hydride abstraction, which then facilitates nucleophilic attack by hydroxylamine. This results in the highly selective formation of B(12) oxygen derivatives of the $[CB_{11}H_{12}]^-$ anion. Based on these observations, we propose a novel mechanism: oxoammonium oxidation-induced nucleophilic substitution (OINS).

Finally, we employed various N–O compounds for the reaction to verify the universality of the method. All reactions were conveniently set up and conducted under ambient air conditions. Considering that oxoammonium cations can be generated by the disproportionation of nitroxide radicals in acidic media, we attempted to conduct a one-pot reaction by directly employing nitroxide radicals. As shown in Fig. 5, common piperidine nitroxide radicals also worked. Additionally, for some substrates with active groups, moderate to high yields were achieved. Moreover, during the reaction with free radicals, we detected the structure of the hydroxy-oxoammonium adduct, which further proved that the mechanism of the reaction involved free radicals first generating hydroxy-oxoammonium adducts and oxoammonium cations *via* disproportionation. This method enables the construction of similar B–O–N structures with various nitroxide radicals, providing a reference for potential future applications.

Conclusions

In conclusion, we have developed a new strategy to achieve high selectivity B–H functionalization of $[CB_{11}H_{12}]^-$, and an OINS mechanism was proposed. With this approach, a series of novel and stable B–O–N derivatives were synthesized. S_N1 type nucleophilic substitution reactions on aromatic rings have long been recognized as challenging.[51–53] Our research indicates that the successful nucleophilic substitution on the $[CB_{11}H_{12}]^-$ anion is attributed to three primary factors: (1) the B–H bond is more easily cleaved compared to the C–H bond in conventional aromatic systems; (2) oxoammonium cations can abstract the hydride (H^-) due to their unique oxidizing abilities; and (3) the resulting product is a zwitterionic compound, which contributes to its stability. This work establishes a novel regioselective derivatization method and advances the mechanistic understanding of derivatization in aromatic compounds.

Data availability

The data supporting this article have been included as part of the ESI.† All data can be obtained from the authors. Crystallographic data for compounds **2**, **3b**, **4b** and **4c** have been deposited with the Cambridge Crystallographic Data Centre (CCDC) under accession numbers 2407119–247122. The data can be obtained free of charge *via* **https://www.ccdc.cam.ac.uk/data_request/cif**.

Author contributions

H. L. conceived the project and supervised the work with Y. W. and J. Y. W. S. conducted the experiments and drafted the original manuscript. Y. J. contributed to the development of the methodology. Y. W. performed theoretical calculations. Z. W. participated in the experimental design. J. S. provided critical feedback and assisted in data analysis. S. D. offered constructive comments. All authors discussed the results, reviewed, and contributed to the final manuscript.

Conflicts of interest

There are no conflicts to declare.

Acknowledgements
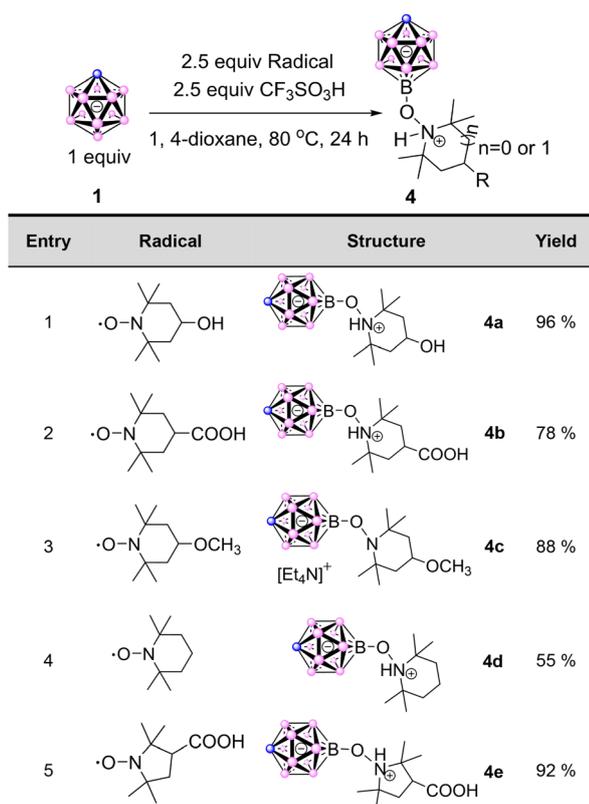
Fig. 5 Substrate scope of B(12) derivatives.

Notes and references

1 A. J. Baublis and A. M. Spokoyny, *Chem*, 2024, **10**, 29–32.

2 R. J. Grams, W. L. Santos, I. R. Scorei, A. Abad-Garcia, C. A. Rosenblum, A. Bita, H. Cerecetto, C. Vinas and M. A. Soriano-Ursua, *Chem. Rev.*, 2024, **124**, 2441–2511.

3 A. D. Ready, Y. A. Nelson, D. F. Torres Pomares and A. M. Spokoyny, *Acc. Chem. Res.*, 2024, **57**, 1310–1324.

4 W.-B. Yu, P.-F. Cui, W.-X. Gao and G.-X. Jin, *Coord. Chem. Rev.*, 2017, **350**, 300–319.

5 Z. Qiu and Z. Xie, *Chem. Soc. Rev.*, 2022, **51**, 3164–3180.

6 H. A. Mills, J. L. Martin, A. L. Rheingold and A. M. Spokoyny, *J. Am. Chem. Soc.*, 2020, **142**, 4586–4591.

7 J. Wang, L. Xiang, X. Liu, A. Matler, Z. Lin and Q. Ye, *Chem. Sci.*, 2024, **15**, 4839–4845.

8 M. Chen, J. Xu, D. Zhao, F. Sun, S. Tian, D. Tu, C. Lu and H. Yan, *Angew. Chem., Int. Ed.*, 2022, **61**, e202205672.

9 A. Marfavi, P. Kavianpour and L. M. Rendina, *Nat. Rev. Chem*, 2022, **6**, 486–504.

10 P. Stockmann, M. Gozzi, R. Kuhnert, M. B. Sárosi and E. Hey-Hawkins, *Chem. Soc. Rev.*, 2019, **48**, 3497–3512.

11 A. W. Tomich, J. Chen, V. Carta, J. Guo and V. Lavallo, *ACS Cent. Sci.*, 2024, **10**, 264–271.

12 P. F. Cui, X. R. Liu and G. X. Jin, *J. Am. Chem. Soc.*, 2023, **145**, 19440–19457.

13 S. O. Gunther, Q. Lai, T. Senecal, R. Huacuja, S. Bremer, D. M. Pearson, J. C. DeMott, N. Bhuvanesh, O. V. Ozerov and J. Klosin, *ACS Catal.*, 2021, **11**, 3335–3342.

14 L. Wang, S. Wu, J. Hu, Y. Jiang, J. Li, Y. Hu, Y. Han, T. Ben, B. Chen and Y. Zhang, *Chem. Sci.*, 2024, **15**, 5653–5659.

15 K. Zhang, K. Cao, J. Sun, Y. Jin, J. Liu and S. Duttwyler, *Inorg. Chem.*, 2024, **63**, 16595–16599.

16 P. Ragué Schleyer and K. Najafian, *Inorg. Chem.*, 1998, **37**, 3454–3470.

17 R. Dontha, T. C. Zhu, Y. Shen, M. Wörle, X. Hong and S. Duttwyler, *Angew. Chem., Int. Ed.*, 2019, **58**, 19007–19013.

18 M. Nava, I. V. Stoyanova, S. Cummings, E. S. Stoyanov and C. A. Reed, *Angew. Chem., Int. Ed.*, 2013, **53**, 1131–1134.

19 D. Olid, R. Núñez, C. Viñas and F. Teixidor, *Chem. Soc. Rev.*, 2013, **42**, 3318–3336.

20 G. E. Dwulet and M. A. Juhasz, *Inorg. Chem. Commun.*, 2015, **51**, 26–28.

21 J. Pecyna, B. Ringstrand, S. Domagała, P. Kaszyński and K. Woźniak, *Inorg. Chem.*, 2014, **53**, 12617–12626.

22 A. Himmelspach, G. J. Reiss and M. Finze, *Inorg. Chem.*, 2012, **51**, 2679–2688.

23 Y. Shen, Y. Pan, K. Zhang, X. Liang, J. Liu, B. Spingler and S. Duttwyler, *Dalton Trans.*, 2017, **46**, 3135–3140.

24 S. V. Ivanov, A. J. Lupinetti, S. M. Miller, O. P. Anderson, K. A. Solntsev and S. H. Strauss, *Inorg. Chem.*, 1995, **34**, 6419–6420.

25 I. Krossing and I. Raabe, *Angew. Chem., Int. Ed.*, 2004, **43**, 2066–2090.

26 C. Douvris and J. Michl, *Chem. Rev.*, 2013, **113**, 179–233.

27 S. Kim, J. W. Treacy, Y. A. Nelson, J. A. M. Gonzalez, M. Gembicky, K. N. Houk and A. M. Spokoyny, *Nat. Commun.*, 2023, **14**, 1671.

28 V. I. Bregadze, I. D. Kosenko, I. A. Lobanova, Z. A. Starikova, I. A. Godovikov and I. B. Sivaev, *Organometallics*, 2010, **29**, 5366–5372.

29 D. Zhao and Z. Xie, *Chem. Sci.*, 2016, **7**, 5635–5639.

30 B. Grüner, I. Císařová, J. Čáslavský, B. Bonnetot and D. Cornu, *Collect. Czech. Chem. Commun.*, 2002, **67**, 953–964.

31 T. Jelínek, B. Stíbr, F. Mares, J. Plesek and S. Hermanek, *Polyhedron*, 1987, **6**, 1737.

32 S. Kőrbe, P. J. Schreiber and J. Michl, *Chem. Rev.*, 2006, **106**, 5208–5249.

33 L. Wang, Y. Jiang, S. Duttwyler, F. Lin and Y. Zhang, *Coord. Chem. Rev.*, 2024, **516**, 215974.

34 P. Kaszynski and B. Ringstrand, *Angew. Chem., Int. Ed.*, 2015, **54**, 6576–6581.

35 J. Pecyna, P. Kaszyński, B. Ringstrand, D. Pociecha, S. Pakhomov, A. G. Douglass and V. G. Young, *Inorg. Chem.*, 2016, **55**, 4016–4025.

36 T. Sahana, A. Mondal, B. S. Anju and S. Kundu, *Angew. Chem., Int. Ed.*, 2021, **60**, 20661–20665.

37 Y. Wang, J. Liu, W. Sun, Y. Zhou, X. Wang, Q. Hu, Z. Wen, J. Yao and H. Li, *J. Org. Chem.*, 2024, **89**, 2440–2447.

38 Z. Lu, M. Ju, Y. Wang, J. M. Meinhardt, J. I. Martinez Alvarado, E. Villemure, J. A. Terrett and S. Lin, *Nature*, 2023, **619**, 514–520.

39 C. Gerleve and A. Studer, *Angew. Chem., Int. Ed.*, 2020, **59**, 15468–15473.

40 W. Wang, X. Li, X. Yang, L. Ai, Z. Gong, N. Jiao and S. Song, *Nat. Commun.*, 2021, **12**, 3873.

41 J. M. Bobbitt, A. L. Bartelson, W. F. Bailey, T. A. Hamlin and C. B. Kelly, *J. Org. Chem.*, 2014, **79**, 1055–1067.

42 D. Leifert and A. Studer, *Chem. Rev.*, 2023, **123**, 10302–10380.

43 J. M. Bray, S. M. Stephens, S. M. Weierbach, K. Vargas and K. M. Lambert, *Chem. Commun.*, 2023, **59**, 14063–14092.

44 Y. Wang, Z. Wen, J. Liu, W. Sun, W. Sun, Q. Hu and H. Li, *Eur. J. Org Chem.*, 2024, **27**, e202400867.

45 Y. Cheng, J. Rein, N. Le and S. Lin, *J. Am. Chem. Soc.*, 2024, **146**, 31420–31432.

46 H. Ren, P. Zhang, J. Xu, W. Ma, D. Tu, C. S. Lu and H. Yan, *J. Am. Chem. Soc.*, 2023, **145**, 7638–7647.

47 S. Liu, J. Tang, F. Ji, W. Lin and S. Chen, *Gels*, 2022, **8**, 46.

48 J. Ding, X. Ding and J. Sun, *Materials*, 2022, **15**, 4498.

49 D. A. Singleton and A. A. Thomas, *J. Am. Chem. Soc.*, 1995, **117**, 9357–9358.

50 K. B. Wiberg and L. H. Slaugh, *J. Am. Chem. Soc.*, 1958, **80**, 3033–3039.

51 R. Glaser, C. J. Horan, E. D. Nelson and M. Kirk Hall, *J. Org. Chem.*, 1991, **57**, 215–228.

52 C. Tang, J. Zhang and Z. Xie, *Angew. Chem., Int. Ed.*, 2017, **56**, 8642–8646.

53 C. Tang, J. Zhang, J. Zhang and Z. Xie, *J. Am. Chem. Soc.*, 2018, **140**, 16423–16427.